EA#ST02-064/ECS02-29 first revised version

Electrooxidation of H_2, CO and H_2/CO on Well Characterized Au(111)-Pd Surface Alloys

T.J. Schmidt[*,1], V. Stamenkovic, N.M. Markovic[*], P.N. Ross, Jr.

Materials Sciences Division, Lawrence Berkeley National Laboratory, University of California, Berkeley, CA 94720, USA

[*] Corresponding authors: schmidt_tj@web.de; nmmarkovic@lbl.gov

[1)] present address: Celanese Ventures GmbH, D-65926 Frankfurt, Germany

Abstract

Electroooxidation of H_2, CO and 1000 ppm CO/H_2 oxidation, were studied on two well defined Au(111)-Pd surface alloys prepared and characterized in ultra high vacuum. Preparation was done using Pd vapor deposition. Characterization was done using Auger electron spectroscopy and low energy ion scattering). After deposition, Pd always (partly) diffuses into the Au(111) crystal and forms stable surface alloys. Two surface alloys with Pd surface concentrations of ca. 38 % and 65 % were transferred into the electrochemical environment. Three major findings from the electrocatalytic study can be summarized as follows: *(i)* hydrogen oxidation on Au(111)-Pd surface alloys is ca. one order of magnitude slower as compared to Pt(111); *(ii)* Au(111)-Pd surface alloys show finite and stable activity for the continuous oxidation of pure CO at potentials below 0.2 V with a positive reaction order with respect to solution phase CO; *(iii)* the oxidation of 1000 ppm CO in H_2 at potentials below 0.2 V is governed by the slow H_2 oxidation kinetics and the unfavorable partial pressure dependence. At potentials above 0.2 V, however, the steady state activity of a high surface area Au-Pd catalyst can be reached.

1. Introduction

Studies on monometallic single crystals and well-defined bimetallic alloy surfaces play a vital role in the understanding of basic surface processes and the electrocatalysis of simple electrochemical reactions such as the hydrogen oxidation (HOR) or the CO oxidation reaction. Numerous recent studies have shown that kinetic investigations on well-defined surfaces can be used to model the electrocatalytic behavior of more realistic high-surface area catalysts used, for example, in low-temperature fuel cell gas-diffusion electrodes. Examples of such studies are H_2, CO oxidation and the oxidation of CO/H_2 mixtures on well-defined bimetallic surfaces (*e.g.*, Pt_3Sn, Pt_xRu_y, Pt_xMo_y, etc. [1-3]) and the corresponding carbon supported high surface area fuel cell catalysts [4-6]. In this communication, we present results for Au(111)-Pd surface alloys and the corresponding supported catalyst. Instead of electrochemical deposition of Pd onto the Au(111) single crystal as proposed in previous studies from other laboratories in order to prepare epitaxial Pd surface layers, see, *e.g.*, ref. [7-9], we decided to prepare the Au(111)-Pd surfaces in ultra-high vacuum (UHV) by means of Pd vapor deposition with subsequent surface characterization by low-energy ion scattering and Auger electron spectroscopy. Rather than forming epitaxial monolayers of Pd on Au(111), as proposed for the electrochemical deposition case [7-9], the UHV preparation methods indicated the formation of real Au-Pd surface alloys [10,11] which was also observed when Au and Pd are electrochemically co-deposited onto Au(111) [12]. Formation of Au-Pd surface alloys is an important factor for mimicking the properties of realistic AuPd catalysts towards the oxidation of H_2, CO, and CO/H_2 mixtures [13]. After description of the preparation and characterization of the Au(111)-Pd surfaces in UHV, we

will present results on the oxidation of the three aforementioned reactions using the rotating disk electrode (RDE) technique. Additionally, a comparison with the properties of PdAu/carbon catalysts will given with respect to the CO tolerance of these electrode surfaces.

2. Experimental

The preparation and characterization of the Pd modified Au(111) electrodes (hereafter denoted as Au(111)-Pd) in a UHV chamber was fully described previously [11]. In short, after several Ar^+-sputtering/annealing cycles, the cleanliness of the surfaces were checked by Auger electron spectroscopy (AES, 3 keV). Subsequently, the crystal was cooled to liquid nitrogen temperature (77 K) and the surface was modified with different amounts of Pd by means Pd vapor deposition. Note that an eventually present Au(111)-22 x $\sqrt{3}$ surface reconstruction is lifted during the deposition of 'multilayer' amounts of Pd [14]. The deposition of Pd was followed by simultaneously recording the AES signal for Pd at 330 eV in a range of ±10eV. After deposition the total coverage of Pd was determined by low energy ion scattering (LEIS). LEIS spectra were taken with a He^+ beam energy of 1 keV with sample current from 5 to 30 nA at residual He pressure of $2.5 \cdot 10^{-8}$ Torr. After Pd deposition, the crystal was allowed to thermally equilibrate with room temperature (ca. 5-6 hours) and the surface composition was checked several times. Once the surface composition of the Au(hkl)-Pd surface alloy electrodes was found to be stable, normally after ca. 24 hours, the crystals were transferred into disk position of a RRDE-setup (*Pine Instruments*) and immersed into the Ar-purged (*Bay Gas Research Purity*) 0.1 M $HClO_4$ (*Baker Ultrex*) electrolyte under potential control (0.2 V RHE). A circulating

constant temperature bath (*Fischer Isotemp Circulator*) maintained the temperature of the electrolyte within ± 0.5 K. All measurements were conducted nonisothermally, *i.e.*, keeping the temperature of the reference electrode constant (≈ 298 K) while that of the working electrode was varied between 293 K and 333 K. The reference electrode was a saturated calomel electrode (*SCE*) separated by a closed electrolyte bridge from the working electrode compartment in order to avoid chloride contamination. All potentials, however, refer to that of the reversible hydrogen electrode in the same electrolyte. H_2 (*N6.0*), CO (*N4.5*) and 1000 ppm CO/H_2 were purchased from *Spectra Gases.*

3. Results

3.1 Ex-Situ Characterization of Au(111)-Pd

In order to modify Au(111) with Pd, we prepared two electrodes where an equivalent of 2 and 4 ML palladium, respectively, were deposited. Under the given experimental conditions, we never were able to form a pseudomorphic Pd monolayer on the Au(111) surface as reported for electrochemical Pd deposition on Au(111) [7,8,15,16], except at liquid nitrogen temperature (77 K). However, during thermal equilibration from ca. 77 K to room temperature, Au(111)-Pd surface alloys were formed. Even the deposition of an equivalent of 2 ML and 4 ML Pd onto the Au(111) crystal always leads to the formation of stable surface alloys, see figure 1b and 2b. Careful analysis [17] of the He^+ LEIS spectra after thermal equilibration resulted in a Pd surface concentration of ca. $x_{Pd,\,s} \approx 0.65$ (figure 1b) and $x_{Pd,\,s} \approx 0.38$ for equivalents of 2 ML and 4 ML, respectively. These results strongly suggest that surface alloy formation occurs under our

deposition conditions. The phenomenon was previously observed in ref. [10] and theoretically predicted [18].

The AES spectra of the same electrodes (figure 1a and 2a) clearly show the presence of Pd in the surface as well as the absence of carbon species, pointing to the cleanliness of the sample surface before and after the Pd deposition. We mention in passing that the tendency to form surface alloys was markedly more visible on the more 'open' Au(100) surface [11] in agreement with new results from Pd-electrodeposition [19]. The UHV-prepared Au(111)-Pd surface alloys were subsequently transferred into the electrochemical cell.

3.2 Electrochemical Characterization of Au(111)-Pd

Cyclic voltammetry

In order to characterize electrochemically the Au(111)-Pd electrodes with $x_{Pd,\,s} \approx 0.65$ (figure 1c) and $x_{Pd,\,s} \approx 0.38$ (figure 2c), we recorded the base voltammetry in 0.1 M $HClO_4$ (293 K, 20mVs^{-1}). Compared with pure Au(111) in 0.1 M $HClO_4$ [20], significant H_{upd} formation can be observed on both Pd containing Au(111) electrodes. Interestingly, careful integration of the H_{upd} region leads to values of ca. 145 μCcm^{-2} ± 5 %and ca. 90 μCcm^{-2} ± 5 % for the electrodes with $x_{Pd,\,s} \approx 0.65$ and $x_{Pd,\,s} \approx 0.38$, respectively, which based on the surface atomic density of Au(111) ($1.39 \cdot 10^{15}$ atoms cm^{-2} or 222 μC cm^{-2} based on 1e$^-$ discharge) would result in H_{upd} coverages of ca. 0.65 ML and 0.41 ML H_{upd}. Under the assumption that on every Pd surface atom one H_{upd} is formed, the H_{upd} coverages are almost quantitatively identical with the Pd concentration in the surface determined by LEIS, *i.e.*, a $\Theta_{Hupd} : x_{Pd,\,s}$ ratio of ca. 1 is found.

However, recently $\Theta_{Hupd} : x_{Pd,\,s}$ ratios well below 1 were found on electrochemically formed Au(111)-Pd surface alloys in sulfuric acid with Pd surface concentrations below 15 % [12] (and on epitaxial Pd monolayers on Au(111) [7,21]). The authors of ref. [12] concluded that on Au(111)-Pd surface alloys H_{upd} cannot be formed on single Pd atoms surrounded by Au (Pd monomers), which are the predominant form of Pd at surface concentrations below ca. 15%, as determined by STM. They concluded that Pd dimers and trimers are needed as critical Pd ensemble sizes for H_{upd} formation [12]. Since we do not know the Pd ensemble size in our study (note that LEIS is only determining the overall surface composition and not the Pd distribution in the surface), we can only speculate that on our surfaces with higher Pd surface concentrations Pd ensembles with more than one atom are formed predominantly. Additionally, Pd containing surfaces are known to strongly bind specifically adsorbing anions (*e.g.*, bisulfate and trace chloride impurities in the electrolyte) [17,22], which may affect the ensemble requirement for H_{upd}.

Hydrogen oxidation

The polarization curves for hydrogen oxidation reaction (HOR) are shown in figures 1d and 2d. The i-E-relationship for Pt(111) recorded under the same experimental conditions is shown as a reference (dashed line) among the families of polarization curves for Au(111)-Pd surfaces with $x_{Pd,\,s} \approx 0.65$ and $x_{Pd,\,s} \approx 0.38$, respectively. Well-defined diffusion limited currents can be observed for the electrode with $x_{Pd,\,s} \approx 0.38$, whereas for the surface with $x_{Pd,\,s} \approx 0.65$ the true diffusion limited currents can be reached only for rotation rates up to1600 rpm. Although our database is limited, the reason for that discrepancy may lay in the enhanced adsorption of

chloride anions on the Pd-rich surface, a phenomenon already observed on PtPd-alloys [17,22,23]. Nevertheless, the HOR on Au(111)-Pd surface alloys obeys significantly slower kinetics than on Pt(111), which is represented by the drastically lower values for the exchange current density, i_0, determined in the micropolarization region [24] as described in detail in our previous publications [25,26] (analysis not shown here). Under our conditions at 293 K, i_0 on Au(111)-Pd is ca. 0.06 $mAcm^{-2}$ and ca. 0.08 $mAcm^{-2}$ for $x_{Pd,\,s} \approx 0.38$ and $x_{Pd,\,s} \approx 0.65$, respectively, roughly one order of magnitude lower as for Pt(111) ($i_0 \approx 0.7$ $mAcm^{-2}$). As expected the HOR kinetics on the Pd-richer surface is slightly faster than on the other Au(111)-Pd surface investigated here. For both Au(111)-Pd surfaces, one single Tafel slope of ca. 220 $mVdec^{-1}$ can be fitted between $0.03 < E < 0.3$ V. Note that for Pt(111) a Tafel slope of ca. 70 $mVdec^{-1}$ is observed in the same potential region in both sulfuric and perchloric acid [25,27]. Combined with the very low values for i_0, these rate parameters indicate a chemical rate determining step in the HOR, most likely the adsorption/dissociation of molecular H_2 on the Pd sites of the Au(111)-Pd surfaces. Recently, slower HOR kinetics were also found on carbon supported PdAu high-surface area catalysts *vs*. Pt/C [13], although there the difference was not as marked as on the (111) oriented single crystal surfaces here. Our own preliminary results on the more open Au(100)-Pd surface alloys with similar Pd surface concentrations showed ca. one order of magnitude faster HOR kinetics than on the (111) oriented surfaces here, indicating that the HOR on Au(hkl)-Pd (as on Pt(hkl) [25]) is probably a structure sensitive reaction with defect sites playing a crucial role for the reaction kinetics. Details for about the structure sensitivity on Au(hkl)-Pd will be published elsewhere.

CO Oxidation

In order to obtain first insight into the capability of Au(111)-Pd surfaces to oxidize CO, we performed CO stripping experiments, figure 3a ($20 mVs^{-1}$, 333 K). The second trace after oxidizing the preadsorbed CO monolayer is shown for comparison (for clarity only the second trace for the surface alloy with 65 % Pd in the surface is shown). As expected, significantly more charge under the stripping peaks is observed for the surface with $x_{Pd,\,s} \approx 0.65$ *vs*. $x_{Pd,\,s} \approx 0.38$. Careful integration of the charge under the CO stripping peaks (corrected for the double layer and OH_{ad} adsorption charges [28]) results in a value of ca. 140 $\mu Ccm^{-2} \pm 5$ % for the surface with 65 % Pd, which corresponds to 0.63 ML CO (based on the surface atomic density of Au(111)) and in a value of ca. 75 $\mu Ccm^{-2} \pm 5$ % for the surface with 38 % Pd, corresponding to ca. 0.33 ML of CO, respectively. The close agreement between the Pd surface concentration in the Au(111)-Pd surface alloys with the CO coverage determined from CO monolayer oxidation virtually points to the fact that CO appears to be adsorbed and oxidized exclusively on the Pd surface sites in the Au-Pd surfaces. Careful inspection of figure 3a shows that the CO stripping peak potential is slightly shifted to more negative values, *viz.*, ca. 0.42 V *vs*. ca. 0.49 V on the surface with the higher Pd surface concentration. These peak maxima are at comparably low potentials with respect to Pt(hkl) surfaces [28], but are in a similar potential range than observed on well-defined PtRu alloys [29,30]. Additionally, significant CO_{ad} oxidation currents can be

observed in the potential region well below the stripping peak, even at potentials below 0.25 V, a favorable fact in the design of CO tolerant electrocatalysts.

Since CO stripping experiments cannot give unambiguous information on the true CO oxidation kinetics, we performed also RDE measurements on the continuous CO oxidation (*i.e.*, continuous CO mass transport to the electrode surface), shown in figure 3b. The CO oxidation currents for Pt(111) is traced for comparison. Quite obviously, in the potential range below ca. 0.5 V significant higher CO oxidation currents are observed on the Au(111)-Pd surface alloys *vs.* Pt(111), whereas above 0.5 V higher currents are measured on the latter surface. On Au(111)-Pd surfaces CO oxidation appears to start almost from the beginning of the sweep at ca. 0.05 V in agreement with differential electrochemical mass spectrometry data for CO_2 formation on PdAu/carbon high surface area catalysts [13]. The surface with the higher Pd content, $x_{Pd,s} = 0.65$, is slightly more active than the Au surface with $x_{Pd,s} = 0.38$. Based on recent DFT calculations [31], the CO adsorption energy seems to be significantly reduced on Au-Pd surfaces *vs.* pure Pd depending of the adsorption site geometry and composition. For instance, hollow adsorption sites with mixed compositions (both Au and Pd surface atoms present) appear to be the sites with the most pronounced decrease in CO adsorption energy [31]. Interestingly, recent in-situ IRRAS data showed that the population of hollow adsorption sites with CO increases with the Pd surface concentration in the Au(111)-Pd surface [12] (on pure Pd, mainly the multifold sites are occupied in both electrochemical and UHV environment [12,32]). Hence, it appears that the capability of Au(111)-Pd to oxidize CO_{ad} can be related to a reduced CO adsorption energy.

In order to get further insight into the reaction mechanism, we measured the CO partial pressure (p_{CO}) dependence, using 100% CO, 50% CO/Ar and 25% CO/Ar under potentiostatic conditions at 0.78 V and 0.88 V. Following the analysis proposed by Gasteiger *et al*. [30], assuming of a simple power law rate equation for CO oxidation, $i = k_{(E)} \cdot (p_{CO})^n$ [30], with $k_{(E)}$ being a potential dependent rate constant, the reaction order, n, with respect to solution phase CO can be determined. Surprisingly, a positive reaction order between 0.2 and 0.3 was found (see table in figure 3b), similar to that observed on Pt_3Sn single crystal surfaces [33] and in contrast to Pt and PtRu electrodes [1]. Although not quantified, the opposite partial pressure dependence of Au-Pd *vs*. PtRu catalysts was previously observed in a study of CO tolerance on supported fuel cell catalysts [13].

In order to assess the true CO tolerance of Au(111)-Pd surface alloys, the potentiostatic oxidation of 1000 ppm CO in H_2 is shown in figure 4. After saturating the surface with CO at 0.025 V, the steady-state activity was recorded after a 20 minutes hold at the respective potential. For comparison, the data are compared to a $Au_{0.45}Pd_{0.55}$/carbon fuel cell catalyst [13]. Note, that the currents in figure 4 are normalized to the geometric surface area although the roughness factor of the electrode with the high surface area catalyst is ca. 5 [13]. Although small, very stable steady state currents were observed on the Au(111)-Pd alloy surfaces already at potentials below 0.2 V. In this potential region, the activities are much higher on the high surface area catalyst than on bulk electrodes with a similar surface composition (even by considering the different electrode roughness). Above ca. 0.25 V similar activities were measured on the smooth surfaces and the high surface area catalyst with the surface alloy with ca. 38 % Pd in the surface

being more active than with 65 % Pd which may point to a slightly higher sensitivity of the latter surface towards CO poisoning in the presence of H_2. The reason for the significant differences in activities below 0.2 V is mainly governed by the sluggish HOR kinetics on the (111) oriented Au-Pd surface alloys. At potentials > 0.2 V the high activity towards 1000 ppm CO/H_2 oxidation can be explained by the fact that in this potential region the HOR seems to 'turn on'. However, as mentioned above, much higher HOR oxidation rates were observed in a preliminary study on Au(100)-Pd surface alloys, which, in turn, would lead to higher reaction rates for CO/H_2 mixtures. Kinetic details will be published in a full paper on Au(hkl)-Pd.

5. Conclusion

We studied hydrogen, CO and 1000 ppm CO/H_2 oxidation, respectively, on two well defined Au(111)-Pd surface alloys prepared and characterized in UHV by Pd vapor deposition and surface sensitive spectroscopy (AES, LEIS). It turned out that under the experimental conditions applied in this study, Pd always diffuses into the Au(111) crystal in order to form stable surface alloys. Two surface alloys with Pd surface concentrations of ca. 38 % and 65 % were transferred into the electrochemical environment. Three major findings can be summarized as follows: *(i)* Hydrogen oxidation on Au(111)-Pd surface alloys is ca. one order of magnitude slower as compared to Pt(111). *(ii)* Au(111)-Pd surface alloys are very active for the continuous oxidation of 100 % below 0.2 V. CO oxidation obeys a kinetic with positive reaction order with respect to solution phase CO. *(iii)* The oxidation of 1000 ppm CO in H_2 at potentials below 0.2 V is governed by the slow H_2 oxidation kinetics and the unfavorable CO partial pressure dependence. At potentials above 0.2 V, however, the steady state activity of a high surface area

Au-Pd catalyst can be reached, which demonstrates the high potential of the Au-Pd system after optimization of hydrogen oxidation kinetics.

Acknowledgements

This work was supported by the Assistant Secretary for Energy Efficiency and Renewable Energy, Office of FreedomCAR and Vehicle Technologies, of the U.S. Department of Energy under Contract No. DE-AC03-76SF00098.

References

1. H.A.Gasteiger, N.Markovic, P.N.Ross, J. Phys. Chem., 99 (1995) 16757.
2. H.A.Gasteiger, N.M.Markovic, P.N.Ross Jr., Catal. Let., 36 (1996) 1.
3. B.N.Grgur, N.M.Markovic, P.N.Ross Jr., J. Phys. Chem. B, 102 (1998) 2494.
4. T.J.Schmidt, H.A.Gasteiger, R.J.Behm, J. New Mat. Electrochem. Sys., 2 (1999) 27.
5. T.J.Schmidt, M.Noeske, H.A.Gasteiger, R.J.Behm, P.Britz, H.Bönnemann, J. Electrochem. Soc., 145 (1998) 925.
6. B.N.Grgur, N.M.Markovic, P.N.Ross Jr., J. Electrochem. Soc., 146 (1999) 1613.
7. M.Baldauf and D.M.Kolb, Electrochim. Acta, 38 (1993) 2145.
8. L.A.Kibler, Kleinert.M., R.Randler, D.M.Kolb, Surf. Sci., 443 (1999) 19.
9. K.Uosaki, S.Ye, H.Naohara, Y.Oda, T.Haba, T.Kondo, J. Phys. Chem. B, 101 (1997) 7566.
10. B.E.Koel, A.Sellidj, M.T.Paffett, Phys. Rev. B, 46 (1992) 7846.
11. T.J.Schmidt, V.Stamenkovic, M.Arenz, N.M.Markovic, P.N.Ross Jr., Electrochim. Acta, 47 (2002) 3765.
12. F.Maroun, F.Ozanam, O.M.Magnussen, R.J.Behm, Science, 293 (2001) 1811.
13. T.J.Schmidt, Z.Jusys, H.A.Gasteiger, R.J.Behm, U.Endruschat, H.Bönnemann, J. Electroanal. Chem., 501 (2001) 132.
14. A.W.Stephenson, C.J.Baddeley, M.S.Tikhov, R.M.Lambert, Surf. Sci., 398 (1998) 172.
15. H.Naohara, S.Ye, K.Uosaki, J. Phys. Chem. B, 102 (1998) 4366.
16. H.Naohara, S.Ye, K.Uosaki, J. Electroanal. Chem., 473 (1999) 2.
17. T.J.Schmidt, N.M.Markovic, V.Stamenkovic, P.N.Ross Jr., G.A.Attard, D.J.Watson, Langmuir, 18 (2002) 6969.

18. E.Christoffersen, P.Liu, A.Ruban, H.L.Skriver, J.K.Norskov, J. Catal., 199 (2001) 123.

19. L.A.Kibler, M.Kleinert, D.M.Kolb, Surf. Sci., 461 (2002) 155.

20. F.Silva, M.J.Sottomayor, A.Hamelin, L.Stoicoviciu, J. Electroanal. Chem., 295 (1990) 301.

21. A.M.El-Aziz and L.A.Kibler, J. Electroanal. Chem., 534 (2002) 107.

22. M.Arenz, V.Stamenkovic, T.J.Schmidt, K.Wandelt, P.N.Ross, N.M.Markovic, Surf. Sci., 523 (2003) 199.

23. V.Climent, N.M.Markovic, P.N.Ross, J. Phys. Chem. B, 104 (2000) 3116.

24. E.Gileadi, *Electrode Kinetics for Chemical Engineers and Material Scientists*, VCH-Publisher (UK), London 1993.

25. N.M.Markovic, B.N.Grgur, P.N.Ross Jr., J. Phys. Chem. B, 101 (1997) 5405.

26. T.J.Schmidt, N.M.Markovic, P.N.Ross Jr., J. Electroanal. Chem., 524-525 (2002) 252.

27. T.J.Schmidt, B.N.Grgur, R.J.Behm, N.M.Markovic, P.N.Ross Jr., Phys. Chem. Chem. Phys., 2 (2000) 4379.

28. N.M.Markovic, B.N.Grgur, C.A.Lucas, P.N.Ross, J. Phys. Chem. B, 103 (1999) 487.

29. H.A.Gasteiger, N.Markovic, P.N.Ross, E.J.Cairns, J. Phys. Chem., 98 (1994) 617.

30. H.A.Gasteiger, N.Markovic, P.N.Ross, J. Phys. Chem., 99 (1995) 8290.

31. P.Liu and J.K.Norskov, Phys. Chem. Chem. Phys., 3 (2001) 3814.

32. A.Sellidj and B.E.Koel, Phys. Rev. B, 49 (1994) 8367.

33. H.A.Gasteiger, N.M.Markovic and P.N.Ross Jr., in J.Garche (Ed.), 4. Ulmer Elektrochemische Tage -Elektrochemie für Energie und Umwelt-, p. 193, Universitätsverlag Ulm GmbH, Ulm, 1997.

Figure Captions

Figure 1: (a) Auger electron spectrum (3keV) of UHV prepared Au(111) (straight line) and Au(111) modified with Pd equivalent to 4 ML (broken line). **(b))** LEIS spectrum of the Au(111) modified with Pd equivalent to 4 ML (He^+, $I_E = 5 \cdot 10^{-2}$ mA, 1 keV), resulting in ca. 65 % Pd in the surface. **(c)** Basic voltammetry of Au(111)-Pd with 65 % Pd in the surface (20 mVs^{-1}, 293 K, 0.1 M $HClO_4$) **(d)** Family of polarization curves for the hydrogen oxidation reaction at different rotation rates (straight line, 20 mVs^{-1}, 293 K, 0.1 M $HClO_4$). The curve for Pt(111) at 2500 rpm is shown for reference.

Figure 2: (a) Auger electron spectrum (3keV) of UHV prepared Au(111) (straight line) and Au(111) modified with Pd equivalent to 2 ML (broken line). **(b))** LEIS spectrum of the Au(111) modified with Pd equivalent to 2 ML (He^+, $I_E = 5 \cdot 10^{-2}$ mA, 1 keV), resulting in ca. 38 % Pd in the surface. **(c)** Basic voltammetry of Au(111)-Pd with 38 % Pd in the surface (20 mVs^{-1}, 293 K, 0.1 M $HClO_4$) **(d)** Family of polarization curves for the hydrogen oxidation reaction at different rotation rates (straight line, 20 mVs^{-1}, 293 K, 0.1 M $HClO_4$). The curve for Pt(111) at 2500 rpm is shown for reference.

Figure 3: (a) CO stripping on Au(111)-Pd for surfaces with 38 % (straight line), and 65 % (dashed line) Pd in the surface (20 mVs^{-1}, 0.1 M $HClO_4$, 333 K). The second trace for Au(111)-Pd with 65 % Pd is shown for comparison. **(b)** Continuous CO oxidation

(2500 rpm) on Au(111)-65 % Pd and Au(111)-38 % Pd (20 mVs^{-1}, 0.1 M $HClO_4$, 333 K). The curve for Pt(111) recorded under identical conditions is shown for reference. **Inset:** Values for the reaction order with respect to solution phase CO on Au(111)-Pd surface alloys.

Figure 4: Potentiostatic oxidation of 1000 ppm CO in H_2 (2500 rpm, 333 K, 20 min at each potential) on Au(111)-65 % (gray diamonds), Au(111)-38 % Pd (gray squares) and a supported $Au_{0.45}Pd_{0.55}$/carbon fuel cell catalyst (extracted from ref. [13].

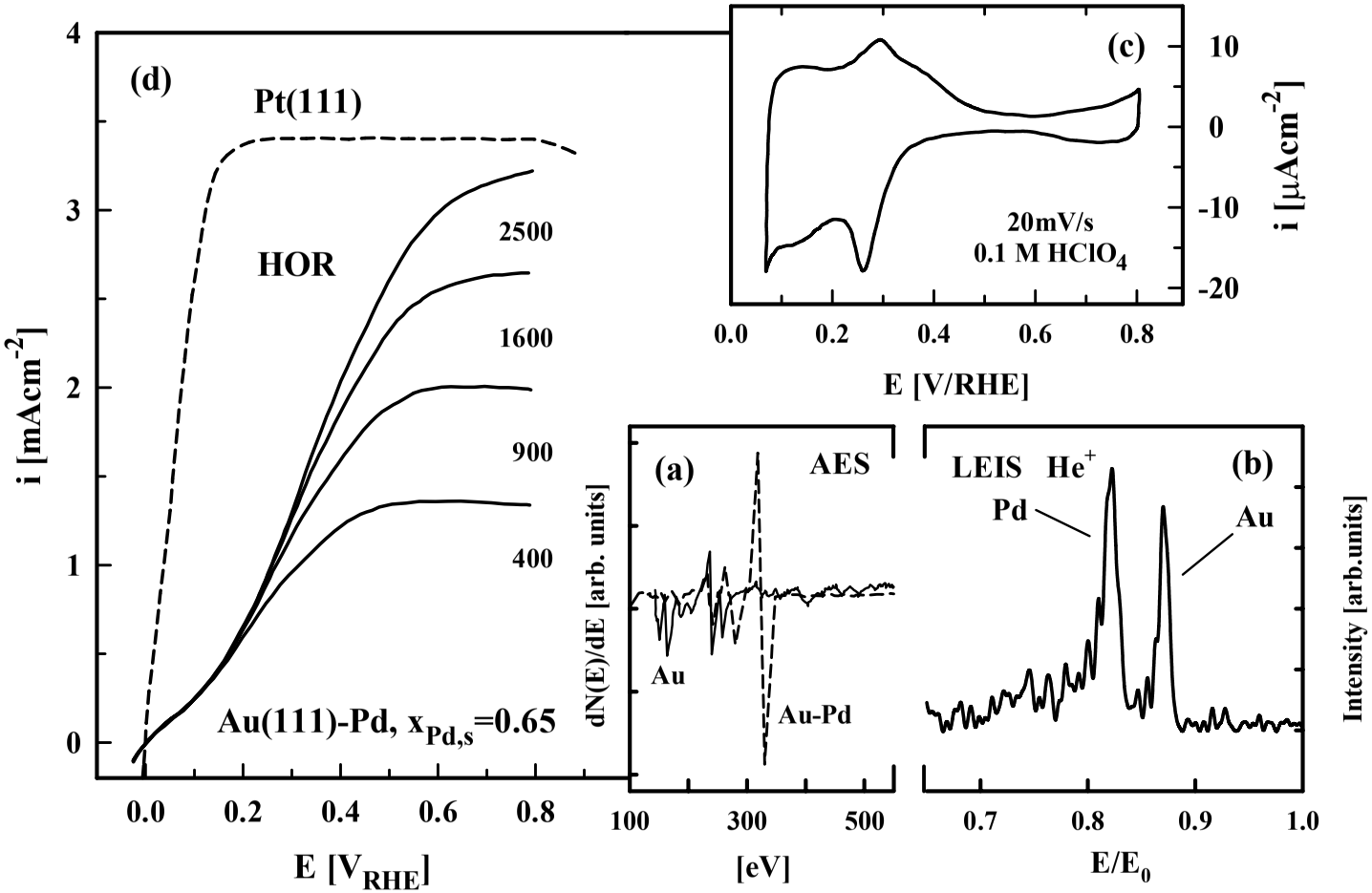

Schmidt et al., figure 1

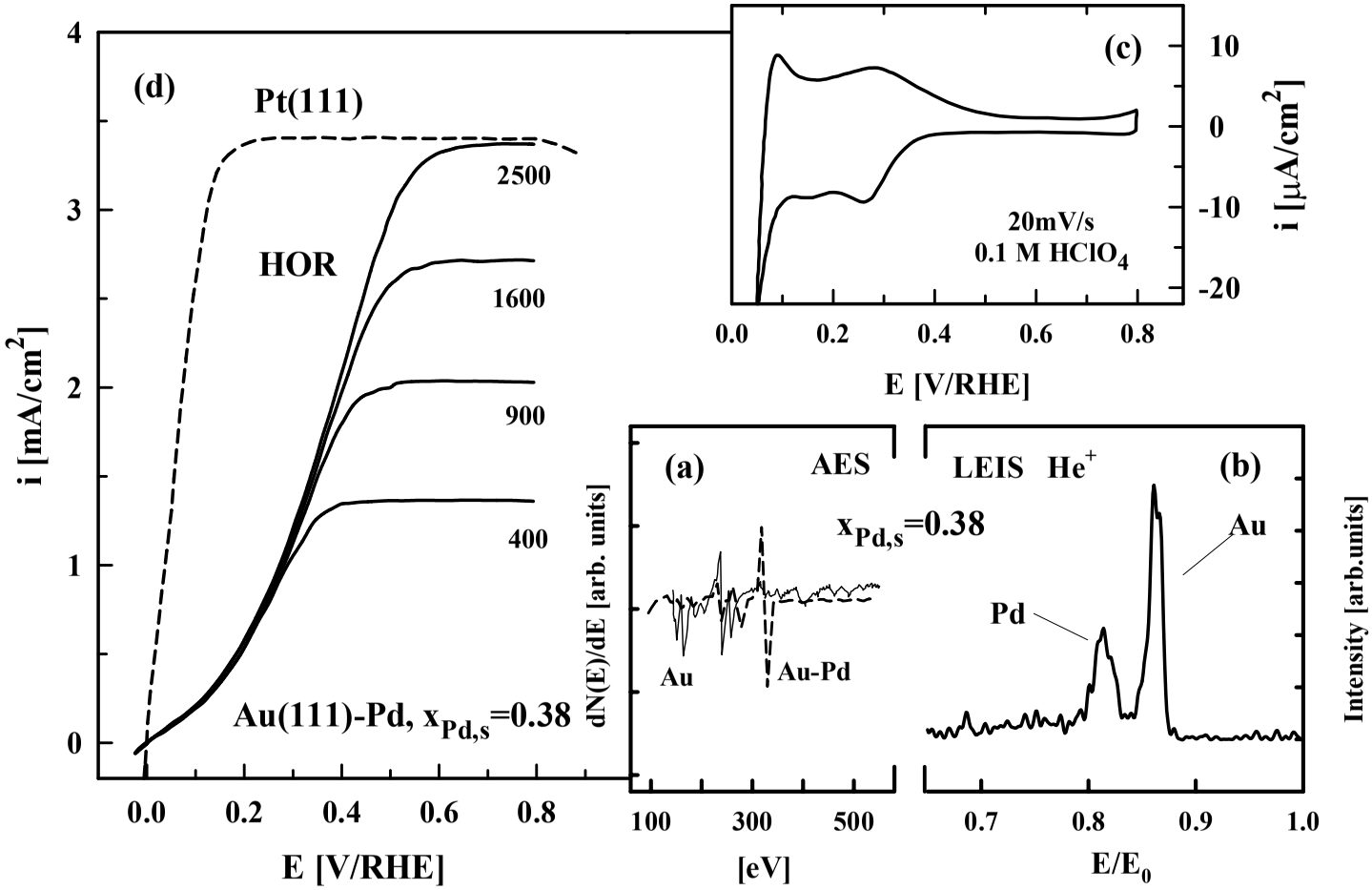

Schmidt et al., figure 2

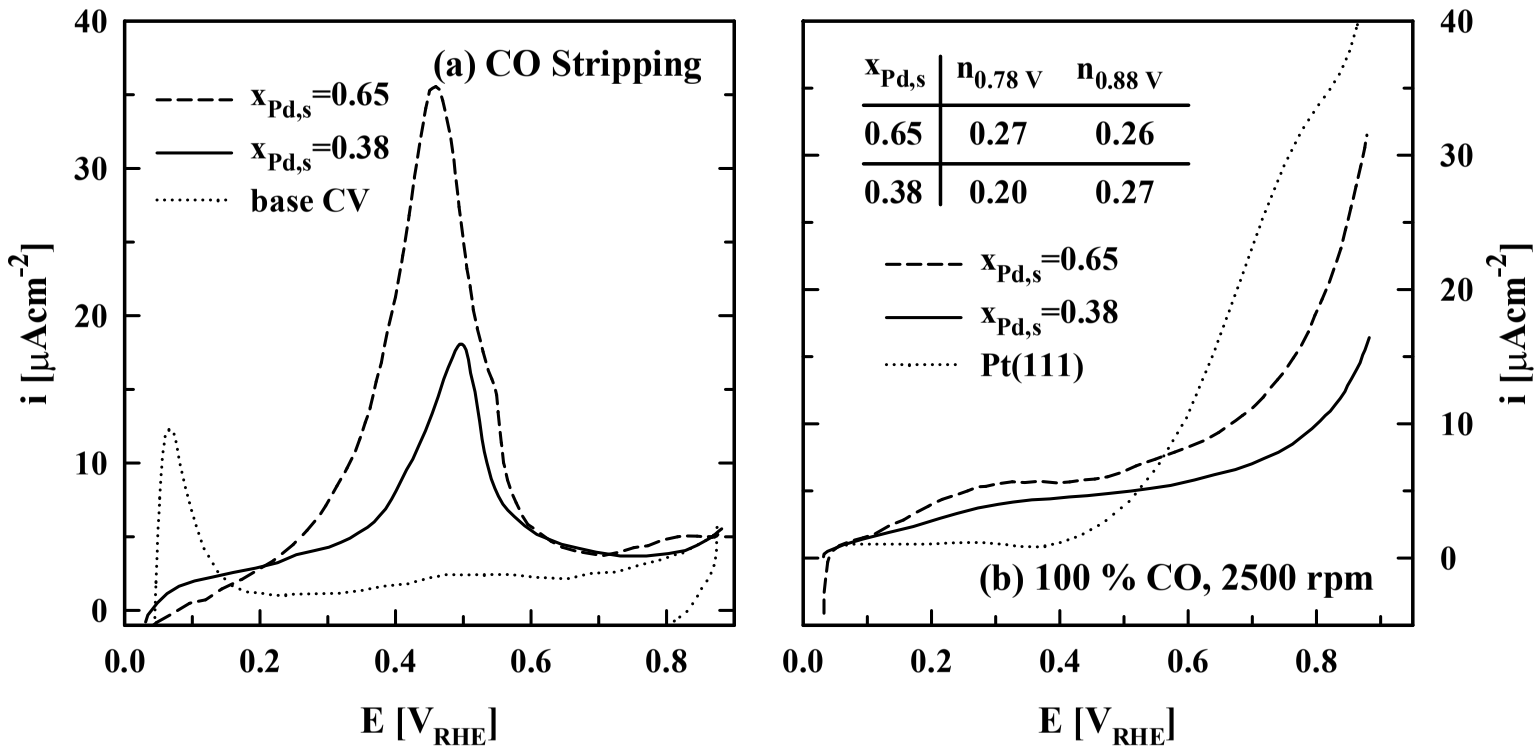

Schmidt et al., figure 3

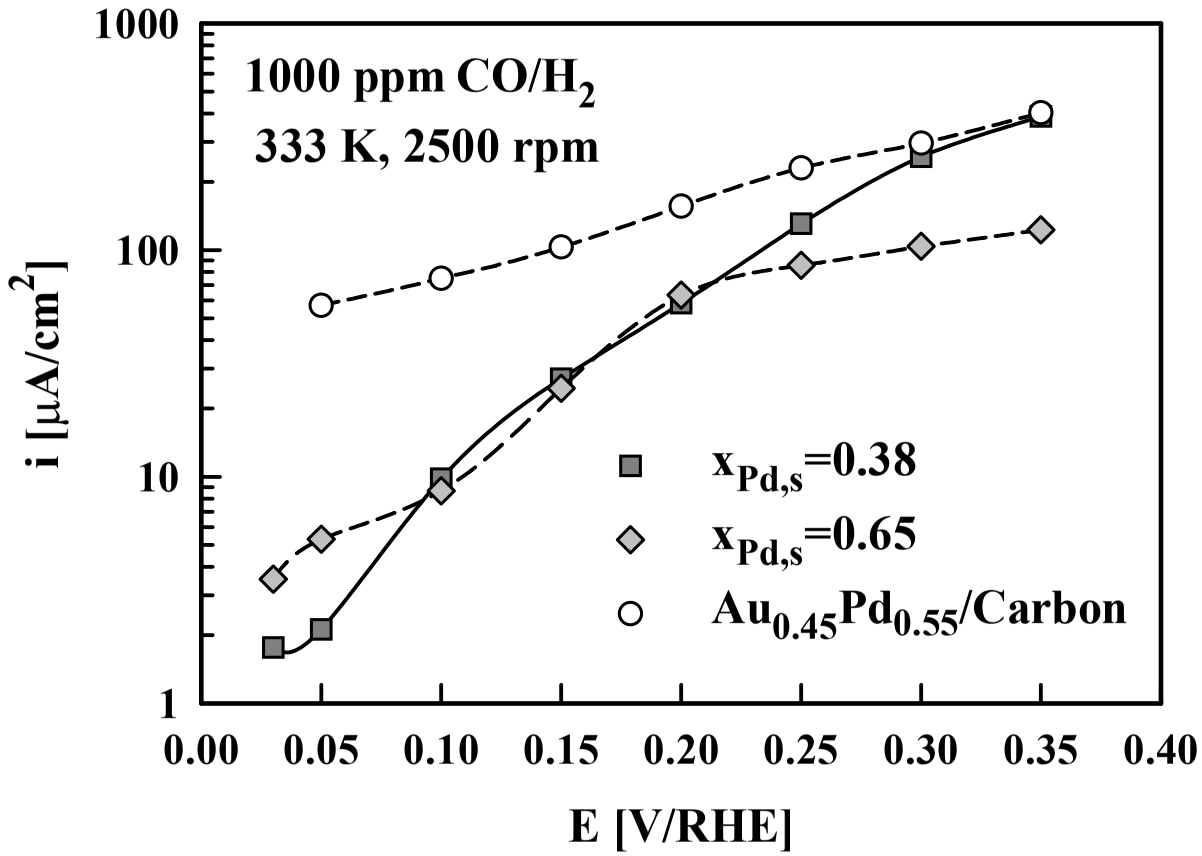

Schmidt et al., figure 4